# Influence of Topography on Forest Reflectance Using Landsat Thematic Mapper and Digital Terrain Data

*C. E. Leprieur* and *J. M. Durand*
Laboratoire d'Etudes et de Recherches en Télédétection Spatiale, 18 Avenue E. Belin, 31055 Toulouse, France
*J. L. Peyron*
Ecole Nationale de Génie Rural, des Eaux et des Fôrets, 14 rue Girardet, 54042 Nancy, France

ABSTRACT: The relationship between forestry variables and the response of Thematic Mapper bands is analyzed over selected mountainous forest sites with a view to improving current models. Forestry stand species and age information was collected for 250 sites in a region with slopes up to 35 degrees and a variety of aspects. Spring and summer Thematic Mapper imagery over the area were used; these data contain a wealth of information related to species and age, and topography. A digital elevation model was compiled with a resolution of 30 metres in order to study the relationship between reflectance, the variable of interest, and the local sun/surface/sensor geometry. Site radiance is dependent on illumination effects and directional effects. The distribution of apparent reflectances versus topographic parameters for each forestry class and each spectral band helped characterize species by their reflective properties. The influence of the age on the apparent reflectance distribution is analyzed : reflectance globally decreases with stand age, especially for TM4, TM5, and TM7.

## INTRODUCTION

LANDSAT DATA have been shown to allow reasonable discrimination of land-use cover types, except in areas of high topographic relief. Different slope angles and orientations cause variable illumination angles and reflection geometry. The resulting effect is readily apparent in Landsat imagery as an impression of local relief. The nature and sources of the topographic effects have been examined by several authors (e.g., Kimes and Kirchner, 1981; Proy, 1986). Current models describing factors controlling directional reflectance and ground illumination fall short of accounting for bidirectional reflectance as derived from Landsat imagery (e.g., Cavayas *et al.*, 1984; Teillet *et al.*, 1982). There have also been a number of studies to develop topographic distribution models which would provide a quantitative description of forest cover types against topographic parameters (e.g., Fleming and Hoffer, 1979; Strahler *et al.*, 1979); but these approaches did not take into account the reflectance distribution with the topography. Previous work in the analysis of Thematic Mapper data related to forest canopy is limited, especially in mountainous areas. Our objectives are a better understanding of the signal components (1) to improve the recognition of forestry variables (e.g., species, ages) in a mountainous area and (2) to quantify the radiometry variation according to the sensor/target/sun position. We analyze the evolution of the signal against various components of the relief in relation to forest variables, then proceed to quantify the influence of the topographic effects.

## STUDY SITE, SPECTRAL AND DIGITAL TERRAIN DATA

### STUDY SITE AND COVER TYPE SELECTION

The Saint Quirin forest study site is located in the mountainous area of Vosges in the east of France. The area contains a diversity of cover types including conifer stands (fir, pine, spruce, and douglas) and deciduous (oak, beech). Each site is characterized by a dominant tree species and mean trunk diameter; the latter parameter is easily measurable and generally associated to the age of the trees by foresters, using an empirical growth formula. Forestry planners in this area have defined 24 forest resource categories for stratification purposes, of which 19 are present on the test site.

The stratification elements are

- dominant species :

| | | |
|---|---|---|
| | (S1) Beech | – Fagus sylvatica L. |
| deciduous | (S2) Oak | – Quercus pedunculata Ehrh., Quercus sessiliflora (Salisb.) Smith |
| | (S3) Fir | – Abies alba Miller |
| conifers | (S4) Pine | – Pinus sylvestris L. |
| | (S5) Spruce | – Picea abies Karsten |
| | (S6) Douglas | – Pseudotsuga Douglasii Carr. |

- tree height : < 3 m – Seedlings (D4)
  > 3 m – trunk diameter
  - < 20 cm – (D3)
  - 20 – 45 cm – (D2)
  - > 45 cm – (D1)

Each of the 381 forest sampling sites was examined on color infrared photographs. Of the 381 stand sites, 250 sites were suitable and were selected for study. They average 88 pixels each. The inner limits of the stand sites were manually registered to a Lambert projection by using a 1:25,000-scale base map (see Table 1).

### IMAGE DATA SELECTION

The Landsat-5 TM data were acquired on 25 April and 30 July 1984, which were the only cloudless acquisitions for that year.

TABLE 1. FORESTRY VARIABLES DISTRIBUTION (SPECIES, AGES) AT THE 250 SAMPLING SITES —SAINT QUIRIN TEST ZONE

| | Species | | | | | | |
|---|---|---|---|---|---|---|---|
| age | S1 | S2 | S3 | S4 | S5 | S6 | all |
| D1 | 5 | 1 | 40 | 6 | 9 | 0 | 61 |
| D2 | 41 | 7 | 45 | 22 | 7 | 0 | 122 |
| D3 | 24 | 2 | 11 | 1 | 0 | 0 | 38 |
| D4 | 13 | 0 | 8 | 4 | 1 | 3 | 29 |
| all | 83 | 10 | 104 | 33 | 17 | 3 | 250 |

S1 = Beech, S2 = Oak, S3 = Fir, S4 = Pine, S5 = Spruce, S6 = Douglas
D1: $\phi \geq$ 45cm, D2: 20 $\leq \phi <$ 45cm, D3: $\phi <$ 20cm, D4: Seedlings.

PHOTOGRAMMETRIC ENGINEERING AND REMOTE SENSING,
Vol. 54, No. 4, April, 1988, pp. 491–496.

0099-1112/88/5404–491$02.25/0

The six reflective TM bands were used. The area of interest was located close to nadir so that parallax displacement can be neglected. Color infrared aerial photographs at 1:13,000 scale were available on the Saint Quirin forest site. These photographs were used in conjunction with ground data from forestry planning to document the canopy.

### Digital Terrain Data

Digital terrain data for the Saint Quirin forest were produced according to the method developed by Proy (1986):

- digitizing the contour lines every 100 metres from 1:50,000-scale maps;
- smoothing the digitized curves;
- interpolating the elevation grid; and
- generating separate images of slope angle, aspect, and cosine of the solar incident angle (i.e., angle between the surface normal and the solar beam).

These images have a resolution of 30 metres.

All these images were registered to the Lambert projection. The elevation varied from 250 to 900 metres with slopes up to 35 degrees.

## DATA PROCESSING AND ANALYSIS

### Processing

A 200 by 2000-pixel block of TM data, including the whole test site (400 by 550 pixels : 200 km$^2$), was extracted from the TM scenes.

*Equalization and geometric correction*. For the six reflective channels the responses of the 16 detectors were different, especially for TM1, TM2 , and TM3 . A statistical equalization of the 16 detectors on the 2000 by 2000-pixel block (equalization of mean values and standard deviations with regard to each statistical distribution) corrected this problem. The new pixel block was registered to the Lambert projection using a geometric resampling algorithm derived from a deformation model (4th degree polynomial) and using 30 control points.

The accuracy of this registration was visually checked by overlaying the shaded relief image and the contour lines of the sampling sites with the Landsat single band images for the two dates.

This procedure was straightforward because the area contains numerous features (clearcuts) which are easily recognized on Landsat images and also because the area has boundaries corresponding to rivers and paths. The correspondence was more obvious between the spectral images and the contour lines of the sampling sites than with the cosine image; the impression of relief was not always closely related to the relief registration.

*Radiometric processing*. We refer to $R$ as the "apparent reflectance" without atmospheric corrections; this notation is better suited for general forestry variable comparisons irrespective of the local sun/surface/sensor geometry.

The reflectance ($R_i$) measured by the satellite is defined by

$$R_i = \frac{\pi \cdot L_i}{Es_i \cdot \cos \theta s}$$

*where* $L_i$ is the upward scattered radiance when the ground is illuminated by the solar incident beam (irradiance : $Es_i$; incident zenith angle : $\theta s$), with $i$ being the band index.

The integrated values of $Es$ over the spectral bands by weighting with the solar flux and the calibration coefficients ($a_{1i}$, $a_{0i}$) to convert digital count ($DC_i$) into radiance ($L_i$) and reflectance ($R_i$) (e.g., Markham and Barker, 1985) are reported in Table 2.

We use

$$L_i = a_{1i} \cdot DC_i + a^o{}_i$$

Then we compute $R_i$ as described above to normalize the data to physical values independent of solar direction and, therefore, of date.

The transformation was made for all bands except for TM1 because the calibration coefficients were not available at that time (see Table 2).

Illumination and directional effects are topography-related: illumination effects depend mainly upon the solar incident angle cosine on each pixel (i.e., angle between the surface normal and the solar beam); directional effects are caused by a modification of the reflectance with solar incident angle ($i$) and observation angle on each pixel ($v$). The term "$R$" is dependent on solar incident angle ($i$), observation angle ($v$, and, strictly speaking, on local illumination (cos $i$) on each point.

### Analysis

In this section Landsat 5 data are evaluated by interpreting digital products and statistical data for selected forestry variables. The effect of topography on apparent reflectance is presented in graphical form and quantitatively described. The summary statistics for each forestry class are presented in apparent reflectance value, i.e. in the [0,1] range.

*Forestry variables analysis*. The correlation matrix (Table 3) and mean values and standard deviations (Table 4) for the TM data on the 250 sampling sites are presented. These summary statistics provide an overview of the relative contribution of the TM spectral bands.

The interband correlation on the forest sampling sites shows a high positive correlation between all bands in April due to the nature of ground cover conditions such as dormant vegetation stands. The situation in July is quite different. We have a high correlation between TM bands 2 and 3 and between TM bands 5 and 7, and low correlation between band 3 and bands 4 and 5. The latter bands are thus best suited for discriminating species or age in full foliage situations. This result is consistent with the selection made by Benson (1985) and Horler (1986) for general forest cover type discrimination.

Between April and July for all species and ages, apparent reflectance decreases in TM2, TM3, TM5 , and TM7 and increases in TM4. In April the differences between species are important because of their different chlorophyll content. Apparent reflectance is greater than 0.070 in TM3 for beech, oak, and douglas (Table 4). This fact could be connected to the phenology because leaves are just coming out or are still missing for deciduous trees and because bare soils are visible through douglas plantations.

The variation of the plant canopy structure (TM4) is greater in July when the foliage is complete than in April.

Absorption of middle infrared radiation (TM5, TM7) is species-dependent with lower reflectance for fir, pine, and spruce than for beech, oak, and douglas in April.

Reflectance decreases for all bands as the age increases (Table 4). the near and middle infrared regions (i.e., TM4, TM5 , and TM7) are very sensitive to stand age or other variables correlated to age such as leaf area or canopy geometry.

Standard deviations are alike for all species and ages whatever the spectral band may be. This fact suggests that species and age discrimination depends on radiometry rather than on radiometry standard deviation.

As for canopy structure, Horler (1986) noted that TM5 and TM7 seemed to be sensitive to forest vegetation density and Butera (1986) to the canopy closure. Because of the absence of diffuse sky illumination, these bands are also sensitive to tree shadows (the apparent reflectance variation exceeded 10 percent for TM5 and TM7 on the test site). This in one of the elements which influence the reflectance of the forest target, as Crist and Cicone (1984) and Horler and Ahern (1986) suggested.

The reflectance variability within classes is such that there is

TABLE 2. VALUE OF THE PARAMETERS USED TO COMPUTE THE APPARENT REFLECTANCE VALUES ON THE TM BANDS.
25 April 1984: $\cos \theta s = 0.7532$
30 July 1984: $\cos \theta s = 0.7906$

| | TM bands | | | | |
|---|---|---|---|---|---|
| $i$ | 2 | 3 | 4 | 5 | 7 |
| $\lambda 1$ (μm) | 0.52 | 0.63 | 0.76 | 1.58 | 2.08 |
| $\lambda 2$ (μm) | 0.60 | 0.69 | 0.90 | 1.79 | 2.35 |
| $Es_i$ (mW/cm$^2$.μm) | 181.26 | 154.60 | 104.67 | 21.11 | 7.69 |
| $a_{1i}$ (mW/cm$^2$.sr.μm.DC) | 0.1175 | 0.0806 | 0.0814 | 0.0108 | 0.005699 |
| $a_{0i}$ (mW/cm$^2$.μm) | −0.2805 | −0.1194 | −0.1500 | −0.0370 | −0.0150 |

TABLE 3. TM BANDS CORRELATION MATRIX ON THE 250 FORESTRY SAMPLING SITES FOR THE TWO DATES.

| | 25 April 1984 | | | | | 30 July 1984 | | | | |
|---|---|---|---|---|---|---|---|---|---|---|
| | TMS | TM3 | TM4 | TM5 | TM7 | TM2 | TM3 | TM4 | TM5 | TM7 |
| TM2 | 1.00 | 0.96 | 0.83 | 0.91 | 0.91 | 1.00 | 0.83 | 0.72 | 0.75 | 0.79 |
| TM3 | | 1.00 | 0.79 | 0.93 | 0.94 | | 1.00 | 0.43 | 0.59 | 0.74 |
| TM4 | | | 1.00 | 0.81 | 0.77 | | | 1.00 | 0.87 | 0.71 |
| TM5 | | | | 1.00 | 0.98 | | | | 1.00 | 0.91 |
| TM7 | | | | | 1.00 | | | | | 1.00 |

TABLE 4. MEAN VALUES/STANDARD DEVIATIONS FOR SPECIES (ALL AGES COMBINED) AND AGES (ALL SPECIES COMBINED). 25 APRIL 1984 AND 30 JULY 1984.

| 25 April 1984. | TMS | TM3 | TM4 | TM5 | TM7 |
|---|---|---|---|---|---|
| S1 | 0.075/0.008 | 0.075/0.014 | 0.206/0.031 | 0.162/0.047 | 0.093/0.033 |
| S2 | 0.083/0.007 | 0.083/0.012 | 0.225/0.028 | 0.191/0.038 | 0.110/0.029 |
| S3 | 0.063/0.009 | 0.054/0.015 | 0.168/0.032 | 0.096/0.048 | 0.049/0.033 |
| S4 | 0.066/0.011 | 0.058/0.018 | 0.168/0.031 | 0.103/0.055 | 0.055/0.038 |
| S5 | 0.066/0.008 | 0.058/0.013 | 0.173/0.026 | 0.106/0.042 | 0.056/0.030 |
| S6 | 0.075/0.009 | 0.073/0.016 | 0.201/0.028 | 0.154/0.050 | 0.089/0.035 |
| D1 | 0.063/0.009 | 0.055/0.014 | 0.166/0.031 | 0.100/0.046 | 0.052/0.031 |
| D2 | 0.068/0.011 | 0.062/0.018 | 0.183/0.037 | 0.122/0.060 | 0.066/0.040 |
| D3 | 0.072/0.009 | 0.071/0.016 | 0.204/0.032 | 0.150/0.054 | 0.085/0.037 |
| D4 | 0.077/0.010 | 0.076/0.017 | 0.210/0.028 | 0.165/0.051 | 0.095/0.037 |
| **30 July 1984.** | TMs | TMe | TMr | TM5 | TM7 |
| S1 | 0.062/0.005 | 0.044/0.005 | 0.313/0.058 | 0.135/0.030 | 0.050/0.014 |
| S2 | 0.066/0.005 | 0.047/0.008 | 0.350/0.047 | 0.143/0.025 | 0.052/0.017 |
| S3 | 0.058/0.006 | 0.042/0.007 | 0.218/0.061 | 0.086/0.034 | 0.034/0.017 |
| S4 | 0.059/0.006 | 0.042/0.006 | 0.223/0.070 | 0.089/0.037 | 0.035/0.016 |
| S5 | 0.059/0.004 | 0.042/0.005 | 0.228/0.060 | 0.090/0.031 | 0.034/0.014 |
| S6 | 0.064/0.005 | 0.046/0.005 | 0.258/0.055 | 0.106/0.028 | 0.043/0.013 |
| D1 | 0.058/0.006 | 0.042/0.007 | 0.216/0.060 | 0.090/0.035 | 0.036/0.018 |
| D2 | 0.060/0.006 | 0.042/0.006 | 0.256/0.077 | 0.103/0.040 | 0.038/0.016 |
| D3 | 0.061/0.005 | 0.043/0.004 | 0.298/0.065 | 0.124/0.036 | 0.046/0.015 |
| D4 | 0.066/0.007 | 0.047/0.009 | 0.319/0.064 | 0.137/0.036 | 0.054/0.018 |

S1 = Beech, S2 = Oak, S3 = Fir, S4 = Pine, S5 = Spruce, S6 = Douglas

D1: $\phi \geq 45$cm, D2: 20cm $\leq \phi <$ 45cm, D3: $\phi <$ 20cm, D4: Seedlings.

significant overlap, though each class is composed of a continuum of sizes and ages that has been arbitrarily divided into clusters. We proceed on the assumption that this variability is primarily related to topography.

*Influence of topography and acquisition geometry: representation and interpretation*. Slope and orientation are the most obvious components of the landscape. Elevation is not as important: the altitude range is less than 700 metres in the study area. The deciduous and coniferous pixels were distributed over the full range of slopes and aspects (Figure 1), however coniferous sites were less numerous on flat areas and on south-east slopes.

In the following paragraphs the July data are evaluated and discussed because the foliage is complete on all forest stands.

**Influence of topography on the signal**. Apparent reflectance normalized by the mean, versus aspects for four classes of slopes for TM5 (Figure 2). The curves in the six reflective bands have the same general shape. The number of samples within each of the 72 aspect classes is presented on Figure 1b.

This curve demonstrate a strong anisotropy of reflectance which exhibits a maximum in the solar direction (137°) and a minimum opposite the sun. This could be related to local illumination variations and to a lack of coniferous on southeast slopes.

The anisotropy of this apparent reflectance ratio increases with wavelength: i.e.,

| band | max | min |
|---|---|---|
| TM2 | +6% | −1% |
| TM3 | +8% | −3% |
| TM4 | +10% | −5% |
| TM5 | +15% | −12% |
| TM7 | +18% | −14% |

For TM5 , the ratio increases with the slope in the sun direction. The evolution seems more difficult to understand opposite the sun. This could be partially related to the coniferous predominance over 10° but also to changeable proportions of bare soil, underwood, and wood with various shadows.

We will lay some emphasis on the case of forestry variables in order to draw certain conclusions as to the behavior of coniferous and deciduous stands.

**Influence of topography in function of forestry classes**. Comparing the reflectance ratio distribution of deciduous and coniferous for all ages, we observe that coniferous stands are more dependent on the sun position than deciduous stands, with a maximum in the solar direction, especially for TM4, TM5, and TM7. TM5 is represented on a graph (Figure 3).

The ratio of the apparent reflectance to the mean apparent reflectance on flat areas is presented for coniferous and deciduous

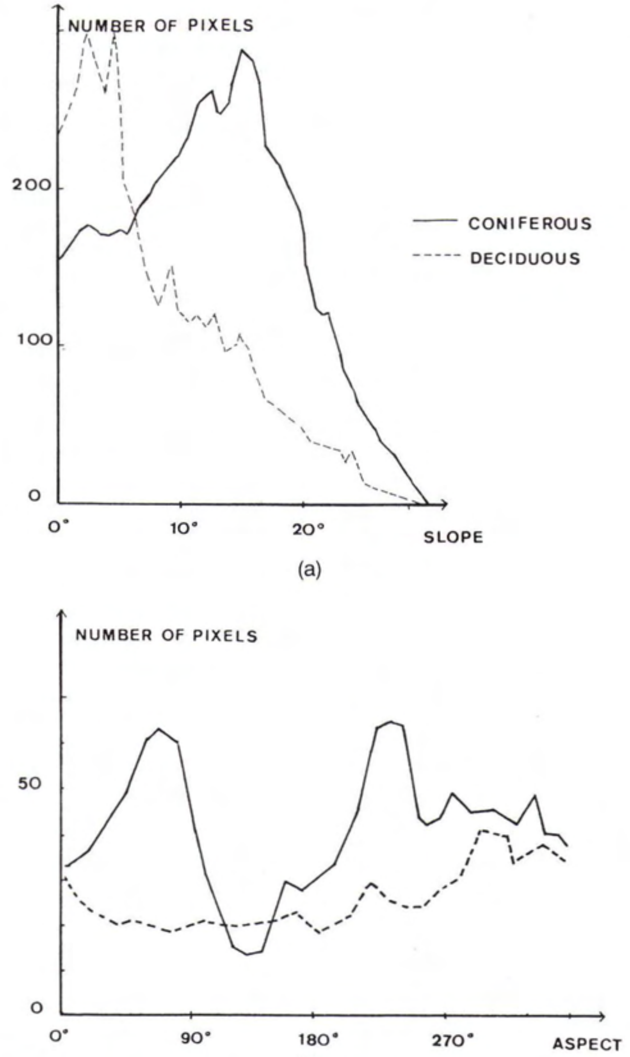


FIG. 1. Species distribution against relief on the St Quirin 250 forestry sampling site: (a) against slope, (b) against aspect.

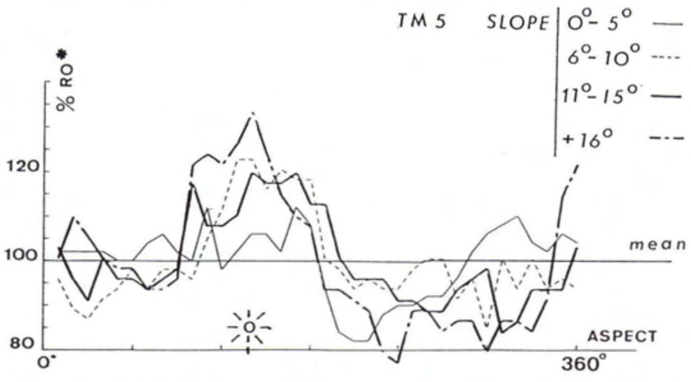


FIG. 2. Apparent reflectance normalized by the mean versus aspects for four classes of slopes for TM5 (250 sampling sites-30 July 1984).

species for TM2, TM3, TM4, TM5, and TM7 (Figure 4). The number of samples within each of the 35 slope classes is represented in Figure 1a.

For coniferous, the signal is below mean for slopes under 18 degrees, especially for long wavelengths (−11 percent for TM5, −14 percent for TM7). On the other hand, the signal increases with respect to mean for slopes between 8 and 20 degrees for deciduous (+5 percent for TM5, +10 percent for TM7). The reflectance variations are smooth, gradually changing functions. They cannot be related to species distribution against slope (Figure 1a), but are probably related to directional and illumination effects.

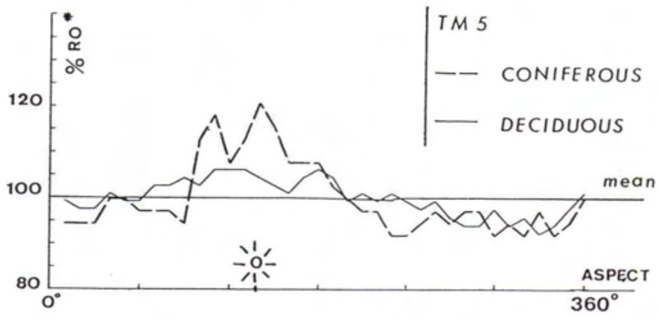


FIG. 3. Apparent reflectance normalized by the mean versus aspects for the two main groups of species (coniferous and deciduous). TM5 represented (30 July 1984).

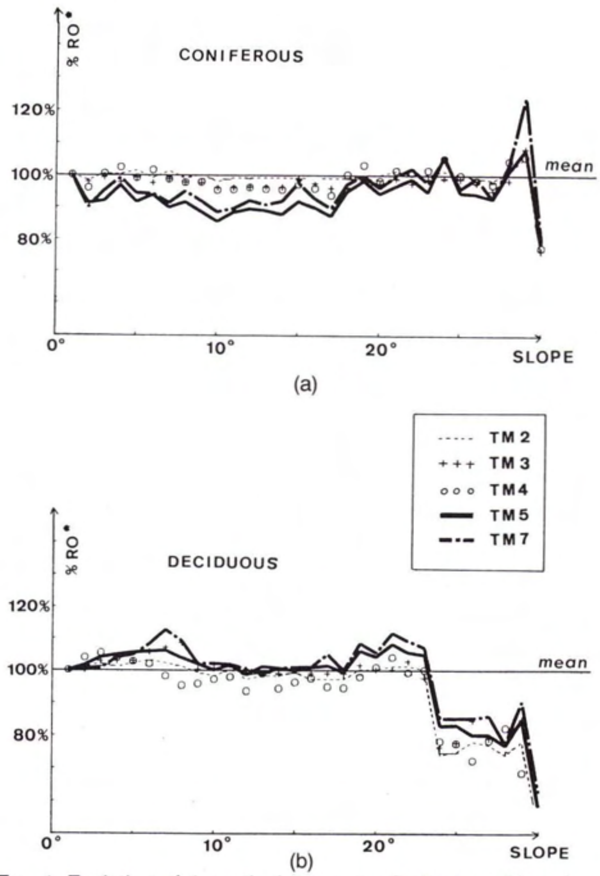


FIG. 4. Evolution of the ratio (apparent reflectance achieved on slopes normalized by the apparent reflectance achieved on flat areas) against the slope (30 July 1984): (a) Coniferous, (b) Deciduous.

The curves do not change sharply over small slope ranges except for the steeper slopes where the number of pixels is small and may not be representative.

The dispersion of the apparent reflectance values (Table 4) is greater for coniferous than for deciduous in these bands excepted for S6 (Douglas) which consists of seedlings. This might be connected with the observations of Kriebel (1978) and Kimes *et al*. (1981) showing a dependence of the reflectance of coniferous forests on sun angle. When stratified by age, the distribution of reflectance ratio is anisotropic. This phenomena is particularly obvious for the older trees (see Figure 5, TM5 represented).

**Synthetic presentations and interpretation.** One of the results of this research is the development of quantitative descriptions of the apparent reflectance distribution, based on geometric and topographic parameters for each forestry variable.

– Distribution of reflectance against *topographic* parameters can be presented graphically in a number of ways. For each species and age involved in this study, a polar diagram of the mean reflectance, which shows the distribution against slope and aspect, is generated. It is possible to analyze the influence of wavelength on these distributions and to compare the reflectance distribution of different groups of species and ages. The polar images such as Figure 6 display the distribution of mean apparent reflectance against aspect (0 to 360 degrees) and slope (0 to 35 degrees) of the surface due to all forestry classes involved in this study. In the TM3, TM4, TM5, and TM7 diagrams, the darker points correspond to the higher values of mean apparent reflectance. The fifth polar diagram illustrates the numbers of pixels used to calculate the mean reflectance for each slope/aspect pair. To document the validity of each value, the number of pixels varies from zero (black) to a maximum (white). This kind of diagram is difficult to represent on a photograph but is easily analyzed on an image analysis system. The linear adaptation of the gray level is different for each band for a better visualization.

– Distribution of reflectance against *geometric* parameters integrates illumination effects. They depend mainly on the local solar incident angle ($i$) defined by the sun direction and the local surface normal.

To account for the different variation sources for species reflectance, it is necessary to study the evolution of the signal against solar incident angle ($i$) and observation angle which is approximately equal to the slope value because of the central position of the test site on the TM scene. An ideal evaluation would account for the fact that the trees do not grow perpendicular to the slope as per the common definition of a bidirectional reflectance distribution function; so we won't refer to this definition because it is not valid here. We can effectively access two variables for each pixel : solar incidence angle and slope. The influence of solar incidence angle on apparent reflectance is presented for each TM band (Figure 7). Reflectance values normalized by mean tend to decrease with solar incidence, the sensitivity increases with wavelength.

The distribution of mean reflectance of three species – beech, fir, and spruce – can be presented with a gray level of depending on the reflectance value in a Cartesian set of axes:

$x$-axis: slope angle (degrees)
$y$-axis: solar incidence angle (degrees)

The values of the mean apparent reflectance are calculated for bands TM3, TM4, and TM5: i.e.,

| | minimum | maximum |
|---|---|---|
| TM3 | 0.026 | 0.065 |
| TM4 | 0.164 | 0.417 |
| TM5 | 0.050 | 0.180 |

In bands TM4 and TM5 the mean apparent reflectance is represented from black (highest value) to pale gray (lowest value) on Figure 8. Reflectance values differ from species to species because of different properties of the biological material and of foliage geometry. The asymmetry of the distribution appears to be species-specific as if each vegetated canopy possessed its own reflection properties.

## CONCLUSION

We have developed a qualitative description of the apparent reflectance distribution for each forestry variable (species and age). A quantitative description of the radiometry variation according to both topographic and acquisition geometry parameters has been provided.

The effects of the sensor/target/sun position are significant on forestry sites. The calculated apparent reflectance values depend strongly on the surface property.

On forestry themes, TM data contain detailed information related to species and stand age. The apparent reflectance values decrease when the stand age increases, particularly for TM4, TM5, and TM7. The discrimination of species is difficult when there are no differences in phenology or foliage geometry.

Because of the great sensitivity of a forest's apparent reflectance to acquisition geometry in the middle infrared part of the spectrum, forestry analysis should take geometry into account. We investigated stand species and ages over the whole angular distribution of reflective properties. We claim that the apparent reflectance data resulting from the processing reported here can help take into account directional reflectance data. Observations such as described here can provide significant information for understanding the factors that affect the spectral response of forestry in mountain areas.

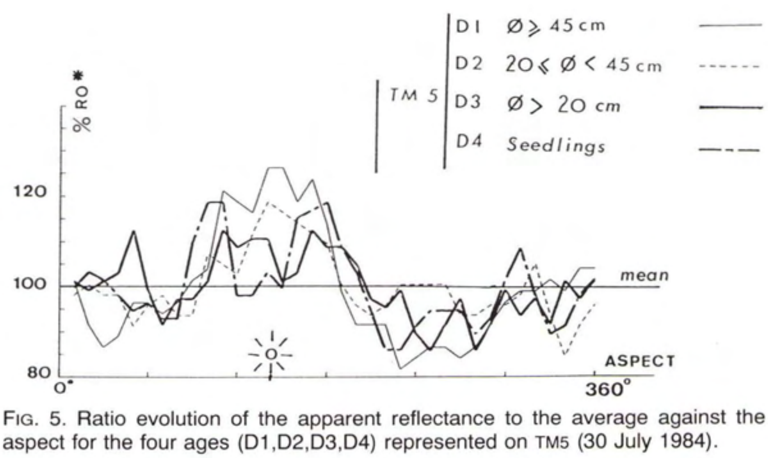


FIG. 5. Ratio evolution of the apparent reflectance to the average against the aspect for the four ages (D1,D2,D3,D4) represented on TM5 (30 July 1984).

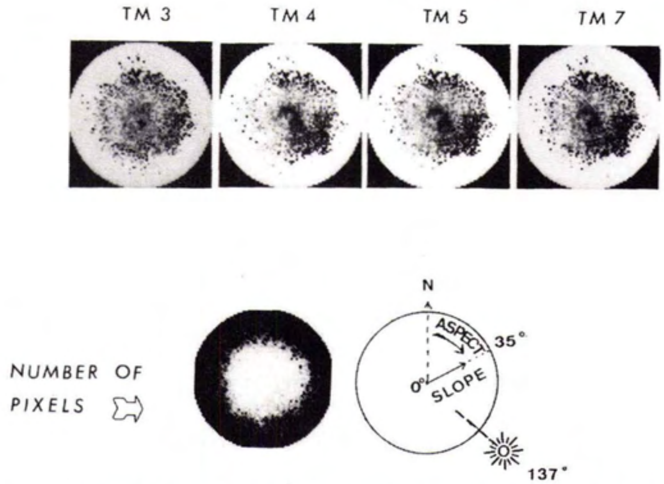


FIG. 6. Polar distribution of the mean apparent reflectance in four TM bands for all the forestry sampling sites (30 July 1984). White = lowest value, black = highest value. Number of pixels represented: white = highest number.

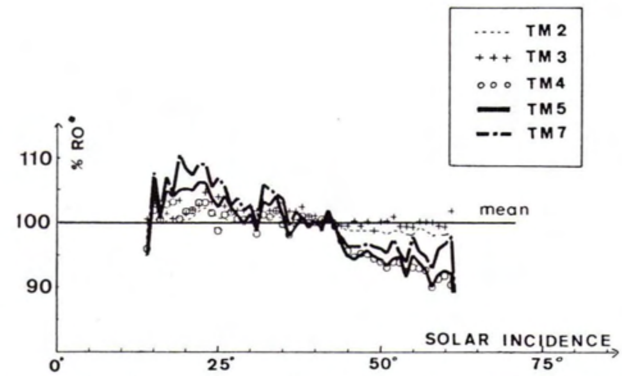


FIG. 7. Apparent reflectance change against the solar incident angle (250 sampling sites) in five reflective TM bands.

## ACKNOWLEDGEMENTS

This research was supported by the "Action Thématique Programmée - C.N.E.S/C.N.R.S.". Contract 85.CNES.1257, CNRS 508533. The authors acknowledge the "Office National des Forèts" - Sarrebourg center - which provided detailed and up to date ground data.

## REFERENCES

Benson, A.S., and S.D. DeGloria, 1985. Interpretation of Landsat-4 Thematic Mapper and Multispectral Scanner Data for Forest Survey, *Photogrammetric Engineering and Remote Sensing*, Vol. 51, No. 9, pp. 1281–1289.

Butera, M.K., 1986. A correlation and regression analysis of percent canopy closure versus TMS spectral response for selected forest sites in the San Juan national forest, Colorado, *IEEE Transactions on Geoscience and Remote Sensing*, Vol.GE-24, No.1, pp. 122–129.

Cavayas, F., G. Rochon, and P. Teillet, 1984. Estimation des réflectances bidirectionnelles par analyse des images Landsat: problèmes et possibilités de solutions, *Proceedings, 8th Canadian Symposium on Remote Sensing, 4e Congrès de l'Association Québécoise de Télédétection*, pp. 645–664.

Crist, E.P., and R.C. Cicone, 1984. A physically-based transformation

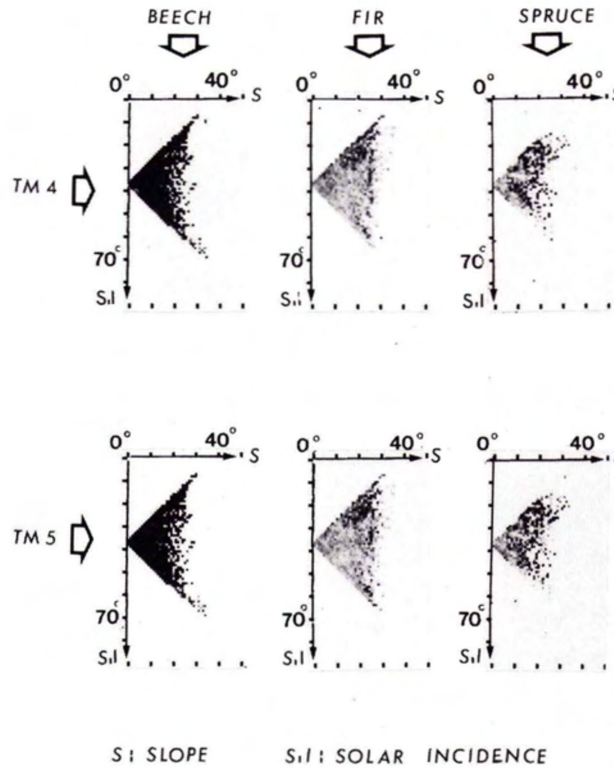


FIG. 8. Mean apparent reflectance distribution for S1(beech), S3(fir) and S4(spruce) in TM3, TM4, and TM5 against:

- $X$ = slope (degrees)
- $Y$ = solar incidence angle (degrees).

White = lowest value, black = highest value.

of Thematic Mapper data - the TM tasseled cap, *IEEE Trans.Geosc.Remote Sensing*, 22, 256.

Fleming, M.D., and R.M. Hoffer, 1979. Machine processing of Landsat MSS data and DMA topographic data for forest cover type mapping, *IEEE Machine processing of Remotely Sensed Data Symposium*, pp. 377–390.

Horler, D.N.H., and F.J. Ahern, 1986. Forestry information content of thematic Mapper data, *Int.J.Remote Sensing*, Vol.7, No.3, pp. 405–428.

Kimes, D., and J. Kirchner, 1981. Modeling the effects of various radiant transfers in mountainous terrain on sensor response, *IEEE Transactions on Geoscience and Remote Sensing*, Vol.19, No.2, pp. 100–108.

Kriebel, K.T., 1978. Measured spectral bidirectional reflection properties of four vegetated surfaces, *Applied Optics*, Vol.17, No. 2, pp. 253–259.

Markham, B.L., and J.L. Barker, 1985. Spectral characterization of the LANDSAT Thematic Mapper sensors, *Int. J. Remote Sensing*, Vol.6, No.5, pp. 697–716.

Proy, C., 1986. *Integration du relief au traitement d'images de télédétection*, D.I. Thesis, Institut National Polytechnique, Toulouse, France.

Strahler, A.H., T.L. Logan, and C.E. Woodcock, 1979. Forest classification and inventory system using Landsat, digital terrain and ground sample data, *Proceedings, 13th Int. Symp. on Remote Sensing of the Environment*, pp. 1541–1557.

Teillet, P.M., B. Guindon and D.G. Goodenough, 1982. On the slopeaspect correction of multispectral scanner data, *Canadian Journal of Remote Sensing*, Vol.8, No.2, pp. 84–106.

(Received 28 July 1986; revised and accepted 7 December 1987)